

In Situ Silica Growth for Superhydrophilic-Underwater Superoleophobic Silica/PVA Nanofibrous Membrane for Gravity-driven Oil-in-water Emulsion Separation

Weihua Qing ^{a,b,§}, Xianhui Li ^{a,§}, Yifan Wu ^a, Senlin Shao ^a, Hao Guo ^a, Zhikan Yao ^a, Yiliang Chen ^c, Wen Zhang ^b,

Chuyang Y. Tang ^{a,*}

a. Department of Civil Engineering, The University of Hong Kong, Pokfulam, Hong Kong 999077

b. John A. Reif, Jr. Department of Civil and Environmental Engineering, New Jersey Institute of Technology, Newark, NJ, 07102, United States

c. College of Biology and the Environment, Nanjing Forestry University, Nanjing 210037, P.R. China

§ Weihua Qing and Xianhui Li contributed equally to this study.

Abstract: Superhydrophilic-underwater superoleophobic (SUS) membranes have been demonstrated to be promising materials for oily wastewater treatment. However, development of facile, low cost and robust SUS membrane with high flux and less membrane fouling is still challenging. In this study, we reported a simple electrospinning/in-situ growth strategy to prepare SUS SiO₂@PVA nanofibrous membrane for gravity-driven separation of oil/water mixture. In specific, a highly porous PVA nanofibrous membrane was first fabricated by electrospinning technique, followed by an in-situ growth of silica nanoparticles on the pristine PVA nanofibers through a modified Stöber reaction. The abundant hydroxyl groups on PVA nanofibers enabled uniform and stable deposition of silica nanoparticles, thus simultaneously realizing high surface energy surface (hydrophilic nature of PVA and silica) and multi-scale roughness. As expected, the resultant membrane exhibited excellent in-air “water-loving” (instantaneous in-air water wetting) and underwater “oil-hating” properties (underwater oil contact angle of 161.8° and sliding angle of 6.2°). The SUS SiO₂@PVA membranes exhibited efficient separation of both free oil/water mixture and a variety of surfactant-stabilized oil-in-water emulsions in a gravity-driven filtration process. In addition, oil density played an important role during the separation process, due to superior separation performance was achieved for lighter-than-water oil when compared to heavier-than-water oils. Moreover, the membrane showed robust

reusability that it maintained stable oil rejection and permeate flux in cyclic experiments.

Key words: Oil/water separation, emulsion separation, superhydrophilic membrane, under-water superoleophobic membrane, silica nanoparticle

1. Introduction

In recent decades, increasing amount of oily wastewater has been generated from frequent oil spill accidents [1, 2] or various industrial processes, such as leather, food, textile, and metal finishing [3, 4]. Therefore, it has become indispensable to purify oil-contaminated wastewater to protect human health and ecological environment. In most cases, oily wastewater exists in the form of oil-in-water emulsion with oil droplets of less than 20 μm . The micro-sized droplet size and good stability of the emulsion, especially those stabilized by surfactants, present huge challenges for efficient oil/water separation. Conventionally, oily wastewater can be separated by gravity or centrifugal settling, chemical or electrostatic demulsification, or biological treatment [5]. However, gravity or centrifugal settling are ineffective for treating emulsified mixtures due to the stabilization of emulsion by surfactants in the mixture, and chemical or electrostatic demulsification methods usually involves high energy consumption and secondary pollution [6]. Therefore, development of an efficient and broadly applicable technique for oily wastewater treatment, especially surfactant-stabilized emulsions, is highly desirable.

Membrane technology exhibits various attractive merits such as low energy cost, small footprint, easy operation and high efficiency [7]. Recently, inspired by lotus leaf's superhydrophobic property, fabrication of porous membrane of special wettability for oil/water separation has gained increasing attention [8]. Wettability is an intrinsic feature of a solid surface which governs the wetting behavior when a liquid contacting with it [9]. If a material displays opposite wetting behavior between oil and

51 water (e.g., superhydrophobic/superoleophilic, or superhydrophilic/superoleophobic), it can realize
52 selective oil/water separation. Up to date, superhydrophobic/superoleophilic membranes for oil
53 removal have been extensively reported for oil-rich oil/water mixture separation [8]. However, this
54 type of “oil-removing” membrane may not work for oily wastewater (e.g., oil-in-water emulsion)
55 separation. For typical oils with lower density than water, water often forms a barrier layer over the
56 membrane surface, preventing oils penetration [10].

57 In this regard, preparation of superhydrophilic-underwater superoleophobic (SUS) membranes
58 as “water-removing” materials have been proposed for oily wastewater treatment [11]. The water
59 droplets can instantaneously wet and penetrate the SUS membrane, and the trapped water in the
60 membrane acts as a superoleophobic barrier to effectively reject oil droplets [12]. Constructing SUS
61 surface generally requires synergy of high surface energy with multi-scale surface roughness [13]. In
62 specific, high surface energy is often realized by using intrinsic hydrophilic materials (e.g., polyvinyl
63 alcohol [14], polyacrylonitrile [15], cellulose [16]) or hydrophilic modification of hydrophobic
64 materials (e.g., polyvinylidene difluoride [17], polytetrafluoroethylene [18]), and multi-scale surface
65 roughness can be constructed by either “top-down” or “bottom-up” strategies [19]. Up to date, a
66 variety of methods (based on grafting [20] or surface coating of polymeric membranes [21], non-
67 solvent phase separation [22], in-situ mineralization of polymeric membranes [23]) have been
68 reported to fabricate SUS membranes for the separation of oil-in-water emulsion. Unfortunately, a
69 major challenge of low permeation flux remains due to low porosities of the SUS membranes in most
70 of the studies.

71 Electrospinning is a promising technique that offers unparalleled advantages to fabricate
72 membranes with high porosity, controllable pore size and thickness. In recent years, increasing efforts
73 have been devoted to fabricate SUS nanofibrous membranes by electrospinning technique for high

74 efficient oil/water separation. The as-prepared nanofibrous membrane offers such a high porosity that
75 often the oil/water separation can be realized solely under gravity. The pristine nanofibrous
76 membranes mostly does not have superhydrophilicity (thus insufficient water affinity to trap water to
77 form the oil repulsive layer [24]), and a second surface roughness enhancement by coating of
78 hydrophilic polymers or inorganic nanoparticles is usually followed to further amplify the “water-
79 loving” property of the membrane for efficient water trapping [13]. These toppings can be coated
80 either by physical deposition (e.g., spraying [25], dip-coating [26], filtration [27]) or chemical
81 modification (e.g., grafting [20], surface polymerization [28], polydopamine binding [29]).
82 Nevertheless, coating by physical deposition often suffers from poor reusability due to the weak
83 noncovalent coating-substrate interactions [30]. To make it worse, severe nanoparticles aggregation
84 often occur due to the high surface energy [31], resulting in poor particle distribution and
85 nanostructure uniformity. Alternatively, though coating by chemical modification offer better
86 reusability, most of existing chemical methods often involves multiple steps (such as surface pre-
87 activation [24], binding layer deposition [14], coating agent pre-synthesis [30, 32]) and expensive
88 raw materials usage. Apparently, development of facile, low cost and robust SUS nanofibrous
89 membrane remains a continuing challenge for efficient oily wastewater treatment.

90 In the present study, we report an eco-friendly SiO_2 @PVA SUS nanofibrous membrane
91 fabricated by a facile electrospinning/In-situ growth strategy for gravity-driven separation of oil-in-
92 water emulsion. PVA is well recognized as a low cost, non-toxic, biocompatible polymer with
93 excellent hydrophilicity, and the abundant hydroxyl groups in PVA molecules readily serve as
94 intrinsic activate sites to facilitate the surface modification [33]. Up to date, PVA-based SUS
95 nanofibrous membrane has yet not been reported for oil/water separation. In specific, a hydrophilic
96 PVA nanofibrous membrane was first fabricated by electrospinning, followed by an in-situ growth of

97 silica nanoparticles on the pristine PVA nanofibers through a modified Stöber reaction. The resultant
98 SiO₂@PVA nanofibrous membrane was systematically characterized to reveal its morphology and
99 chemical component variations when compared to the pristine PVA nanofibrous membrane. Through
100 a variety of wettability measurements, we show that the hybrid SiO₂@PVA nanofibrous membrane
101 exhibit excellent in-air “water loving” and underwater “oil hating” properties. Gravity-driven
102 separation of oil/water mixture were carried out to evaluate the membrane separation performance.
103 Finally, reusability of the SUS membrane was also investigated by conducting cyclic emulsion
104 separation experiments.

105

106 **2. Methodology**

107 **2.1. Materials:**

108 PVA powder (98-99% hydrolyzed, Mw of ~88,000-97,000) was obtained from Alfa Aesar.
109 Tetraethyl orthosilicate (TEOS), ammonia hydroxide (33 wt. % NH₃ in H₂O), glutaraldehyde, ethanol,
110 hydrochloric acid (HCl, 37 wt.%), acetone were all purchased from VWR Chemicals Ltd. Kerosene,
111 n-heptane, toluene, chloroform, Tween 80 were all analytical grade and purchased from Dieckmann
112 chemical industry company limited. All the chemicals were used as received. Milli-Q water with
113 resistivity over 18 MΩ.cm (Millipore, MA) was used in all the experiments.

114 **2.2. SUS SiO₂@PVA nanofibrous membrane fabrication**

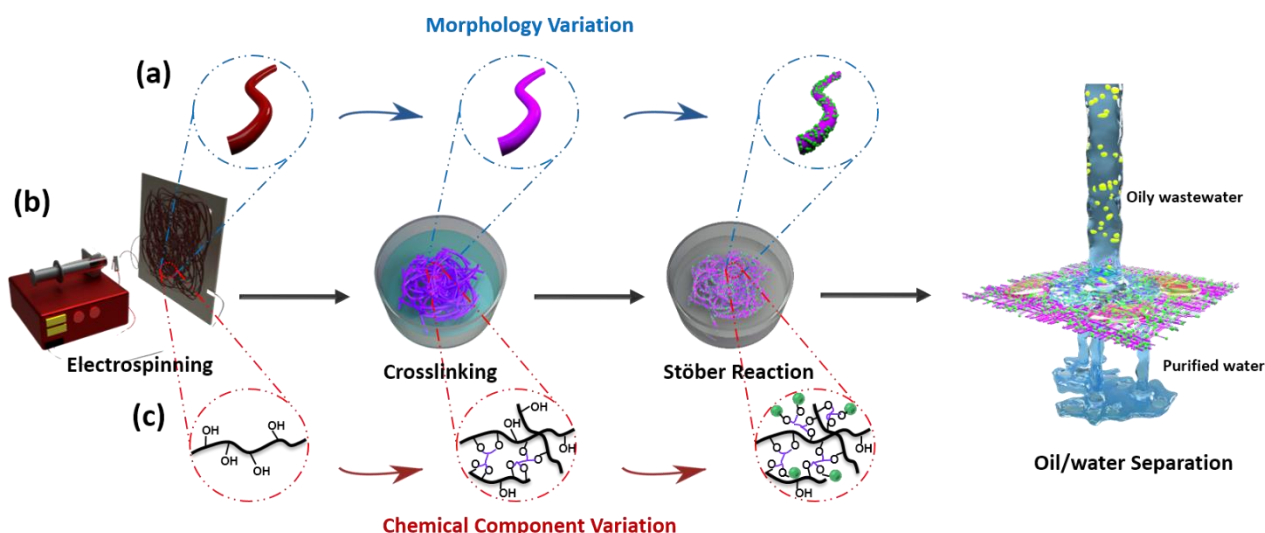


Figure 1. Schematic illustration of the (a) morphology variations during the preparation process, (b) preparation procedure of the SUS SiO₂@PVA membrane, and (c) Chemical component variation during the preparation process.

2.2.1. Hydrophilic PVA nanofibrous membrane fabrication

The fabrication process of SUS SiO₂@PVA nanofibrous membrane is illustrated in **Figure 1b**.

First, a 10 wt.% PVA solution was first prepared by dissolving the polymer in water and stirring the mixture at 90 °C overnight. Afterwards, a PVA nanofibrous membrane was prepared by electrospinning technique with the following conditions: collector/spinneret distance of 15 cm, flow rate of 0.37 mL/h, and applied voltage of 18 kV, drum diameter of 10 cm, drum rotation speed of 80 rpm, and total electrospun PVA solution of 15 mL. Finally, the membrane was cross-linked by immersion the membrane in cross-linking agent containing acetic acid and glutaraldehyde (96/4 v/v) for 0.5 hour, before being dried in the electric oven at 60 °C overnight.

2.2.2. SiO₂ in-situ growth on the PVA nanofibers

Based on the hydrophilic PVA nanofibers, a secondary roughness was created by in-situ growth of SiO₂ nanoparticles on the pristine PVA nanofibers using a modified Stober reaction. First, a small piece of PVA nanofibrous membrane (4×4 cm) was soaked in a flask containing 300 mL ethanol and 30 mL ammonium hydroxide (33 wt.%). The flask was then immersed in an oil bath at 60 °C. Under

133 magnetic stirring, 15 mL TEOS was added into the solution dropwise to start the reaction. After 24
134 hours, the resultant SUS SiO₂@PVA membrane was carefully picked out and rinsed with ethanol and
135 water three times to remove any residual chemicals. Finally, the SUS membrane was dried completely
136 in oven at 60 °C overnight before further use.

137 **2.3. Membrane characterizations**

138 Membrane morphologies were investigated by scanning electron microscopy (SEM) images
139 (LEO1530 FEG SEM). Energy dispersive X-ray (EDX) mapping was also carried out during the SEM
140 measurement to determine the elements distribution on the nanofibers. In addition, mean diameter
141 distribution of membranes was obtained by SEM image analysis using software of Nano Measure
142 System. For chemical component analysis, FTIR-ATR and XPS spectra of the membranes were
143 obtained by Nicolet 8700 (Thermo-Electron, wavenumber range of 4000-500 cm⁻¹) and ESCALAB
144 250 (Thermo Scientific, X-ray source of monochromic Al K α 150 W), respectively. To evaluate the
145 wettability of the membranes, the in air water contact angle, underwater oil contact angle, in air water
146 contacting behavior, and underwater oil contacting behavior were all measured by Attention Theta
147 (Biolin Scientific, Sweden). Note that chloroform was chosen as a model oil for all oil wettability
148 measurements due to its larger density than water. For contact angle measurements, a small droplet
149 (~6 μ L) was deposited on the membrane surface, and allowed for 10 s of stabilization. Average
150 contact angles were calculated from six measurements at different spots of the sample surface.
151 Underwater oil sliding angles were also measured by a goniometer (HWHR Instruments, China).
152 Average membrane thicknesses were also determined by six measurements using a digital caliper.
153 The pore size distribution of the membranes were measured by a capillary porometer (PoroLux™
154 1000, German) using the gas-liquid displacement porometry method [34]. To reflect the membrane
155 porosity, isopropyl alcohol (IPA) uptakes were measured by gravimetric method [35], where the

156 weights of the dry membrane and wet membrane (pre-soaked with IPA solution for over 8 hours)
157 were measured and calculated by the following equation:

$$158 \quad \delta(\%) = \frac{m_w - m_d}{m_d} \times 100 \quad (1)$$

159 where δ is the IPA uptake ($\text{g} \cdot \text{g}^{-1}$), and m_w and m_d are the weight of the dry and wet membranes,
160 respectively.

161

162 **2.4.Oil/water emulsion preparation**

163 Four kinds of surfactant-stabilized oil-in-water emulsion were prepared, including kerosene-in-
164 water (k/w), n-heptane-in-water (h/w), toluene-in-water (t/w), and chloroform-in-water (c/w)
165 emulsions. In specific, 4 mL oils, 0.4 g surfactant (Tween 80), and 200 mL water were vigorously
166 stirred under room temperature for over 8 hours. The resultant milky emulsions were stable with no
167 observation of demixing for at least 24 hours. In addition, free kerosene/water mixture was also
168 prepared with volume ratio of 1:1 to evaluate the free oil/water mixture separation performance.

169

170 **2.5. Gravity-driven oil/water separation tests**

171 Separation of oil/water mixture were performed in a customized dead-end filtration module. In
172 brief, two cylindrical glass tubes were vertically fixed, with a membrane sealed in the middle
173 (effective membrane area of 11 cm^2). To start the separation process, the membrane was first pre-
174 wetted with small amount of water, and then the oil/water free mixture or emulsions were pour into
175 the upper tube. The water spontaneously permeated the membrane and was collected at a bottom
176 beaker. The entire process was driven by gravity without any other external pressure (with a height
177 difference of 6.4 cm, equivalent to a driving pressure of $\sim 0.006 \text{ bar}$). Separation time was recorded

178 to determine the membrane permeate flux, and the oil content in the oil/water mixture and permeate
179 were measured by a total organic carbon (TOC) analyzer (TOC-V CPH, Shimadzu). The oil rejection
180 of the membranes can be calculated using the following equation:

$$181 \quad \eta(\%) = \frac{C_0 - C_p}{C_0} \times 100 \quad (2)$$

182 where η is the oil rejection rate, and C_0 and C_p are the oil content in the oil/water emulsion and
183 permeate, respectively.

184

185 3. Results and Discussion

186 3.1. Membrane surface morphology

187 The morphologies of the membranes were revealed by SEM, and the results are shown in **Figure**
188 **2**. The pristine PVA membrane exhibited a typical morphology of electrospun material, in which
189 nanofibers with mean diameter of 460 nm were interconnected with each other to form a three-
190 dimensional porous structure. However, the surfaces of the PVA nanofibers were very smooth (**Figure**
191 **2a**). After the membrane was treated with a modified Stöber reaction, monodisperse spherical
192 nanoparticles with diameter of ~120 nm were evenly deposited on the pristine PVA nanofibers
193 (**Figure 2b and Figure S1**). Further EDX mapping of single nanofiber revealed that silicon elements
194 were uniformly distributed along the nanofiber (**Figure 2c**), revealing successful deposition of silica
195 nanoparticles by the reaction (further evidences are discussed in the following section). The silica
196 nanoparticles created secondary nanostructures (finer texture) on pristine nanofibrous surface
197 (coarser texture), which, together with their intrinsic hydrophilicity, were expected to amplify the
198 wettability of the membrane from hydrophilicity to superhydrophilicity. Though the mean diameter of
199 the treated nanofibers increased from 460 to 770 nm, and mean pore size slightly decreased from

decreased from 532 ± 3 to 433 ± 5 nm due to the nanoparticles coating, the membrane thickness remained almost unchanged after the treatment (as shown in **Table 1**), which is desirable for a high efficient oil/water separation. In addition, the slight difference of IPA uptakes (**Table 1**) between the treated and pristine membrane implied that the silica coating caused negligible changes to the porosity of pristine membrane.

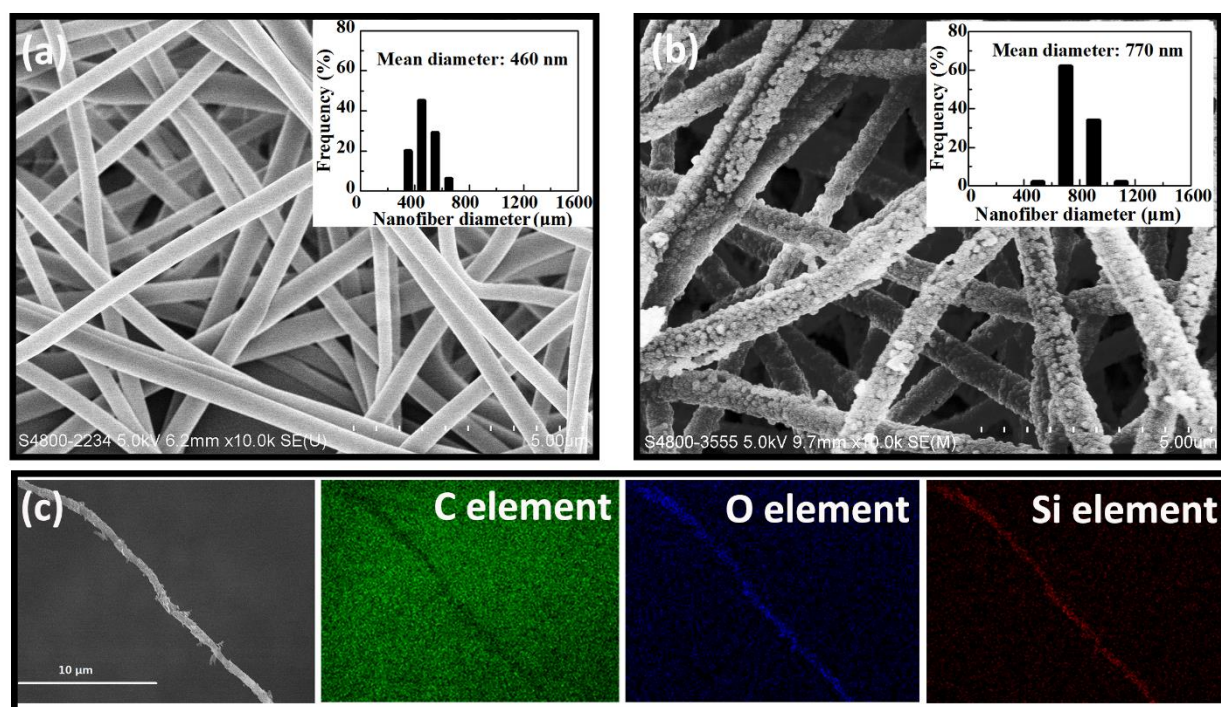


Figure 2. SEM images and corresponding nanofiber diameter distribution of pristine (a) and silica-coated (b) PVA nanofibrous membranes. (c), EDX mapping images of the SiO₂@PVA nanofibrous membrane

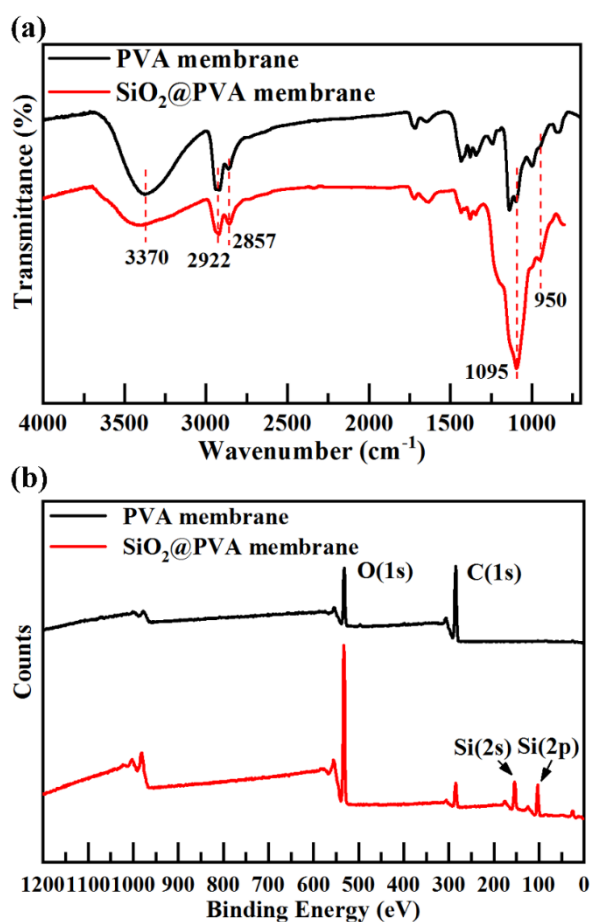
Table 1. Characteristics of the pristine PVA and hybrid SiO₂@PVA nanofibrous membranes

	Mean fiber diameter (nm)	IPA uptake (g·g ⁻¹)	Thickness (mm)	Mean pore size (nm)
Pristine PVA membrane	460±70	4.95±0.02	0.40±0.02	532±3
Hybrid SiO ₂ @PVA membrane	770±90	4.62±0.27	0.39±0.03	433±5

3.2. Chemical analysis

The surface chemistry variation before and after the Stöber reaction were characterized by FTIR and XPS, respectively. In **Figure 3a**, the absorption peak at 3370 cm^{-1} in both spectra were assigned

214 to O-H stretching [36], and the peaks at 2922 and 2857 cm^{-1} were due to the stretching of -CH from
 215 alkyl groups [37]. These absorption peaks verified the presence of PVA. In comparison, new peaks at
 216 1095 and 950 cm^{-1} appeared in the spectra of treated nanofiber, which could be assigned to Si-O-Si
 217 asymmetric stretching [38] and Si-OH stretching [39], respectively. This observation demonstrated
 218 the successful deposition of silica nanoparticles in the treated nanofibrous membrane. In addition, the
 219 abundant hydroxyl groups on the pristine PVA nanofiber surface can form strong hydrogen bonds
 220 with the silanol (Si-OH) group (as illustrated in **Figure 1c**) [40, 41], thus enhanced silica
 221 nanoparticles stability on the nanofibers was expected. Moreover, XPS spectra of both membranes
 222 were presented in **Figure 3b**. Only carbon and oxygen elements were detected in the pristine PVA
 223 membrane, whereas, Si(2s) and Si(2p) signals were detected in the treated membrane, further
 224 confirming the deposition of silica on the PVA nanofibers.



225 Figure 3. Chemical components characterizations: (a), FTIR analysis and (b) XPS analysis of the pristine PVA
 226

3.3. Membrane wettability

The wettability were investigated through in-air contact angle, underwater oil contact angle, as well as dynamic wetting behavior of water or oil droplets on the membranes. In air, the pristine and the treated membranes both had water and oil contact angles of 0°, showing in-air amphiphilicity. When immersed in water, the pristine PVA membrane showed underwater oleophobicity with underwater oil contact angle of 120.6° (**Figure 4a**), however, the oil droplets were sticky on the pristine membrane surface with underwater oil sliding angle of 180°. Remarkably, the SiO₂@PVA membrane exhibited underwater oil contact angle of 161.8° (**Figure 4b**), and underwater oil sliding angle of merely 6.2°, indicating that underwater superoleophobicity was achieved after the silica deposition on the pristine PVA nanofibrous membrane.

The dynamic wetting behavior of water or oil droplets on the membranes were recorded using a high-speed camera. For in-air water wetting process, both the pristine PVA membrane and treated SiO₂@PVA membrane can “capture” the water droplet when the latter touched the membrane surfaces. However, it took almost 7.02 s for the water droplet to completely spread into the pristine membrane (**Figure 4c**), whereas, only 0.53 s was required for the same process on the SiO₂@PVA membrane (**Figure 4d**). More than one order of magnitude improvement in wetting speed was displayed after the silica coating, showing a superior in-air “water-loving” property of the silica decorated PVA membrane. This enhanced water affinity has been demonstrated to one of the key for better oil/water separation performance, because it enable instantaneous water layer formation on the membrane surface to completely reject oil droplets [42].

As for the underwater oil wetting process, one oil droplet was slowly lifted into contact with the

250 membrane surfaces with an obvious deformation, and then lifted away. Remarkably, the oil droplet
251 was dramatically elongated when being lifted up, and eventually deposited on the pristine PVA
252 membrane (**Figure 4e**), indicating a strong underwater adhesion of the oil droplet with the pristine
253 PVA membrane. In contrast, during the same process on the SiO₂@PVA membrane surface (**Figure**
254 **4f**), the oil droplet easily slipped aside due to uneven pressure, and was lifted away from the
255 membrane surface without observable droplet deformation. These observations confirmed a very
256 weak underwater adhesion of the oil droplet (i.e., excellent “oil-hating” property) with the SiO₂@PVA
257 membrane surface, which is highly desirable to reduce membrane fouling [8]: Various previous
258 studies [25, 29, 43] have observed rapid flux drop for using hydrophilic membranes in oil/water
259 separation due to surface pores blockage by strong underwater adhesion of the oil droplet with the
260 membrane surface, whereas superhydrophilic membrane was able to maintain stable separation flux
261 because of the underwater non-sticky property of the membrane towards oil droplet, which will be
262 further confirmed in the following sections. In addition, the enhanced underwater superoleophobicity
263 of the SiO₂@PVA membrane can be attributed to the multiscale roughness created by deposition silica
264 nanoparticles (finer texture) on the pristine nanofibrous surface (coarser texture) [11]. According to
265 Cassie–Baxter theory, when micro/nanostructures are induced on the surface, water can be easily
266 trapped into the hierarchical textures, leading to a composite water-solid interface. In this way, the
267 water trapped in the hierarchically rough structures serves as a repulsive liquid phase to prevent the
268 penetration of the oil droplets, yielding enhanced underwater superoleophobic and low-adhesive
269 properties [8].

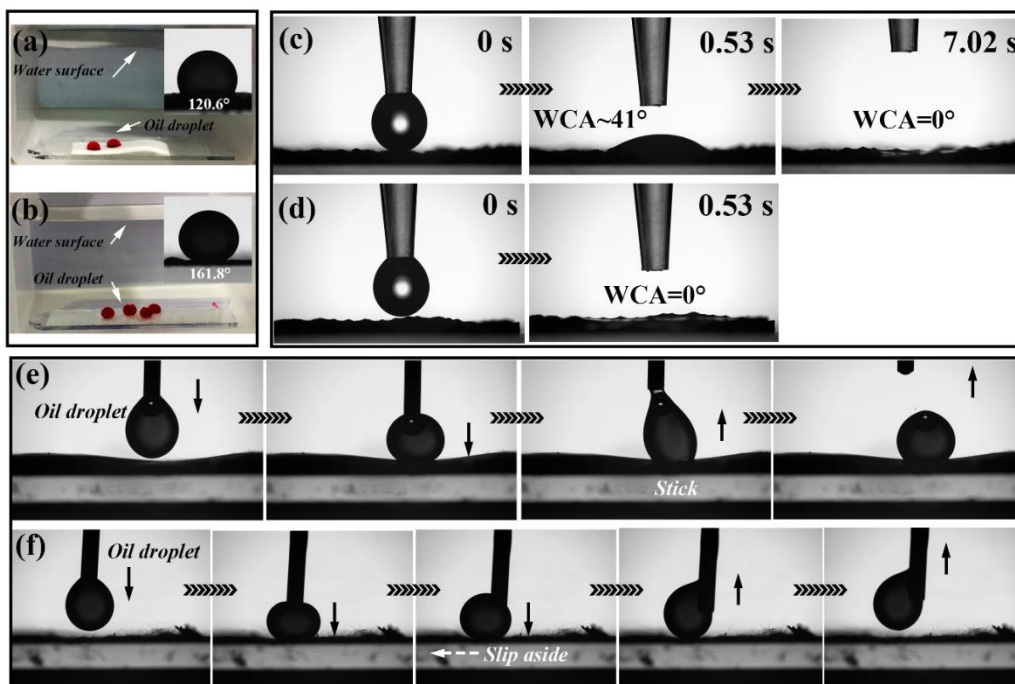


Figure 4. Wettability characterization of the membranes: Under-water oil droplet contact angle on the (a) pristine PVA membrane and (b) SiO₂@PVA membrane, respectively. Snap shots of water droplets spreading on (c) PVA and (d) SiO₂/PVA membrane surfaces. Dynamic underwater contacting behavior of oil droplet with the (e) pristine PVA membrane and (f) SiO₂@PVA membrane.

3.4. Oil/water separation experiments

As evidenced above, the SiO₂@PVA membrane displayed intriguing selective wettability (superhydrophilicity-underwater superoleophobicity) with highly porous membrane structure, which made it an attractive material for oil/water separation application. Therefore, a series of experiments were carried out to evaluate its oil/water separation performances.

First as a proof of concept, free kerosene/water mixture and surfactant-stabilized kerosene-in-water emulsion were separated using the SiO₂@PVA membrane. As shown in **Figure 5a,b**, one prewetted membrane was sealed in the middle of a dead-end model filtration module, and the oil/water mixtures were directly poured into the upper tube. Driven solely by gravity, the water instantaneously wetted the membrane and penetrated into the bottom tube, whereas the oil remained in the upper tube. For both experiments, the penetrates in the bottom tubes were very clear when

287 compared to the initial mixtures, indicating high separation ability. Furthermore, the optical
288 microscopic images of the kerosene-in-water emulsion showed that the initial emulsion was milky
289 with numerous oil droplets dispersed in the water bulk (mean diameter of 1.36 μm), whereas no
290 visible oil droplets were observed in the permeate, further confirming the oil in the surfactant-
291 stabilized emulsion can be efficiently removed by the $\text{SiO}_2\text{@PVA}$ membrane (**Figure 5c**). The same
292 $\text{SiO}_2\text{@PVA}$ membrane was used in recycle kerosene-in-water emulsion separation experiments
293 during which the membrane was simply rinsed with ethanol and water after each cycle. As shown in
294 **Figure 5d**, both the oil rejection and permeate flux remained stable in five cycles of repeated
295 experiments, showing outstanding reusability of the membrane. It can be attributed to the stable silica
296 coating on the PVA fibers (as shown the SEM image of the used membrane in **Figure S2**), which
297 enable the sustained superhydrophilic-underwater superoleophobic properties.

298 In practical processes, oils of different densities can be generated to form emulsified oily
299 wastewater. Herein, the effect of oil density on the oil/water emulsion separation performances was
300 investigated. The model oils were n-heptane, kerosene, toluene, and chloroform with density of 0.684,
301 0.8, 0.867, and 1.49 $\text{g}\cdot\text{cm}^{-3}$, respectively. As shown in **Figure 5e**, for n-heptane, kerosene, and toluene
302 which have lower densities than water, the oil rejections were all over 95% with permeate flux as
303 high as $\sim 1500 \text{ L}\cdot\text{m}^{-2}\cdot\text{h}^{-1}$ under gravity driven of ~ 0.006 bar (This separation performance was much
304 superior than that of conventional micro/ultra filtration membranes [44, 45], and was comparable to
305 recently reported SUS nanofibrous membranes, as shown in **Table 2**). As for chloroform whose
306 density is higher than water, in contrast, both the oil rejection and flux were reduced to 81% and 1159
307 $\text{L}\cdot\text{m}^{-2}\cdot\text{h}^{-1}$, respectively. Clearly, the oil density played an important role during the emulsion
308 separation process, which can be hypothetically illustrated in **Figure 6**. When the light oil whose
309 density was smaller than water approaches the membrane surface during the separation process, it

can easily detach back to the bulk feed due to the non-sticky property of the SUS membrane. In contrast, though also non-sticky, the heavy oil droplets were more likely to rest on the membrane surface due to heavier density, which gradually builds an unfavorable oil accumulation near the membrane surface leading to a reduced permeate flux. To make it worse, the oil droplets whose diameters were smaller than the membrane pore size would have greater chances to permeate the membrane pore, and thus compromised the oil rejection rate.

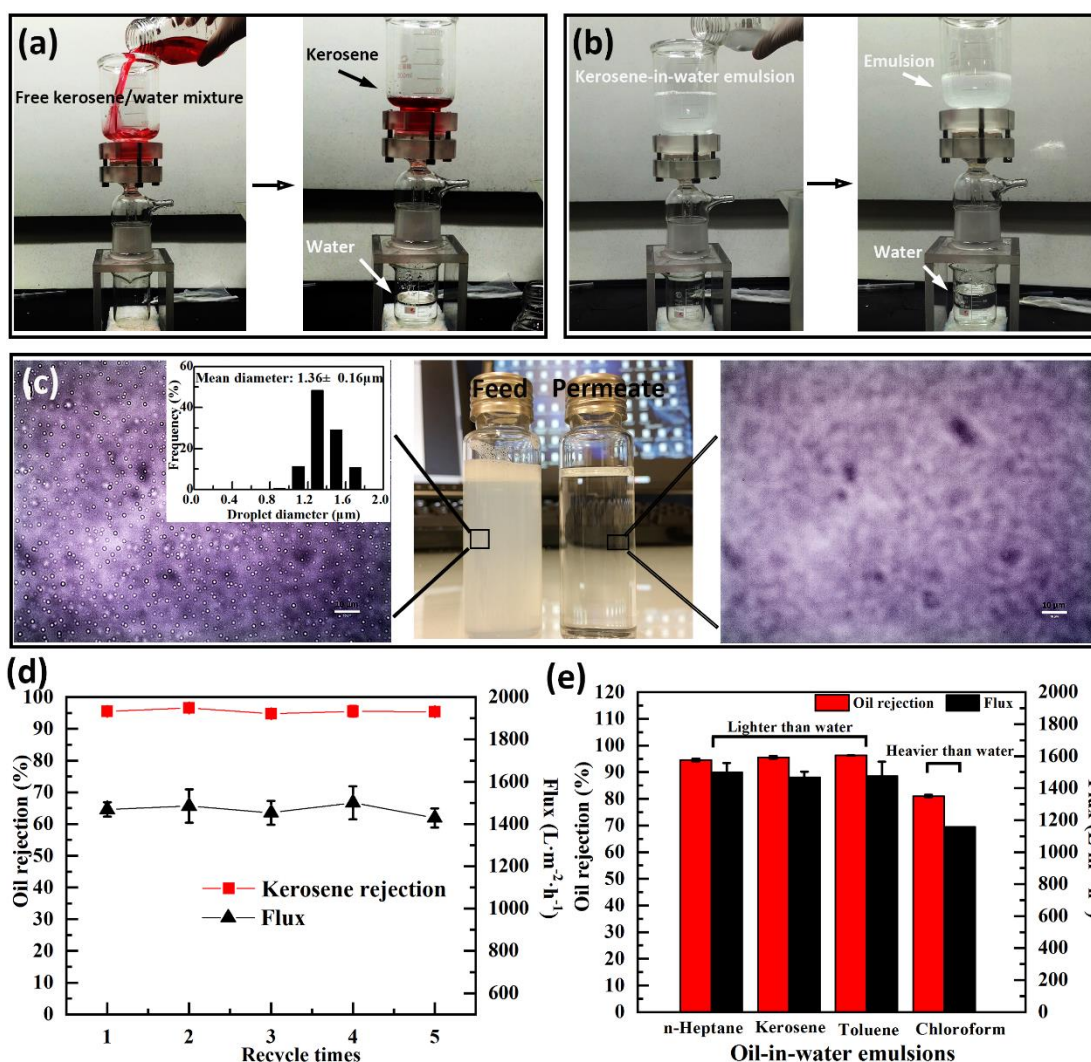


Figure 5. Oil/water separation performances: (a), photos showing free kerosene/water mixture separation process; (b), photo showing kerosene/water emulsion separation process; (c), optical photos of the kerosene/water emulsion and the permeate after separation, the figure inserted at the upper left showed the droplet distribution; (d), oil rejection and separation flux stabilities of kerosene/water emulsion separation using the same $\text{SiO}_2@\text{PVA}$ membrane; (e), oil rejection and separation flux for different oil-in-water emulsion separation processes.

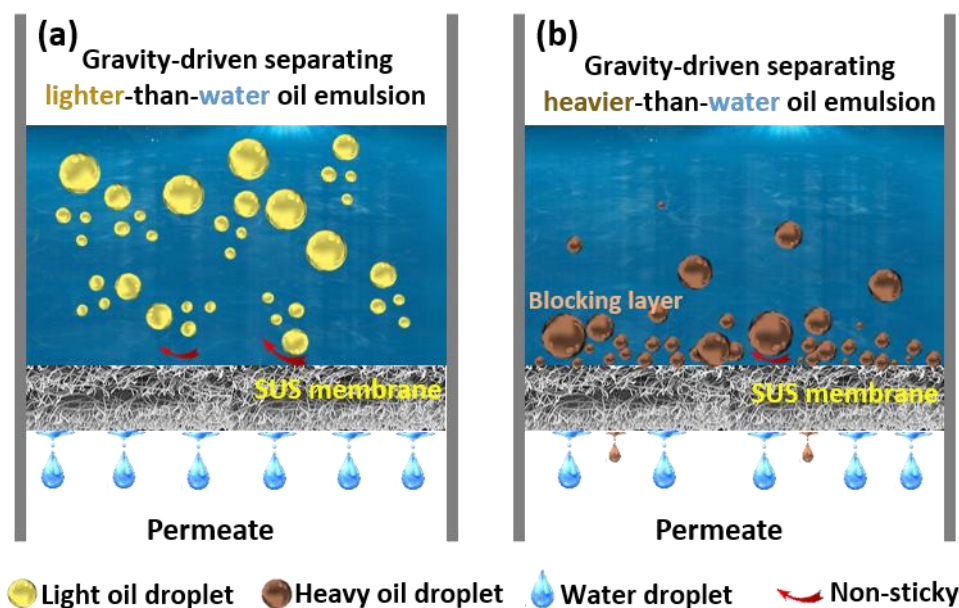


Figure 6. Schematic illustration of different oil/water separation behaviors of (a) lighter-than-water and (b) heavier-than-water oil droplets.

Table 2. Comparison of oil-in-water emulsion separation performances using different nanofibrous membranes

Membrane material	Type	Oil-in-water emulsion	Pressure (bar)	Flux ($\text{L}\cdot\text{m}^{-2}\cdot\text{h}^{-1}$)	Rejection (%)	Publication year and Ref.
P(NIPAAm-co-NMA)/Chitin	Nanofibrous	Edible oil/water	0.3	~1300	99.1	2017, [30]
Composite PAN	Nanofibrous	SDS/n-hexane/water	0.01	692	N.A.	2018, [25]
SiO_2 /PAN/PAN composite	Nanofibrous	SDS/diesel/water	0.01	267	> 96.5	2018, [43]
Clay/PVA	Nanofibrous	DC193 fluid/soybean oil/water	2~6	20~60	> 90	2017, [46]
ZNG-g-PVDF	Nanofibrous	Crude oil/water	N.A.	> 600	> 98.7	2019, [47]
CNT/PAN	Nanofibrous	Tween 20/Canola oil/water	0.2	~60	95	2020, [48]
SiO_2 @PVA	Nanofibrous	Tween 80/toluene/water, Tween 80/heptane/water, Tween 80/kerosene/water	0.006	~1500	> 95	This work

4. Conclusions

In summary, we have reported a simple, low cost electrospinning/In-situ growth strategy to prepare robust superhydrophilic-underwater superoleophobic SiO_2 @PVA nanofibrous membranes for efficient oil/water separation. The pristine PVA nanofibrous membranes are abundant with hydroxyl groups which facilitated in-situ growth of silica nanoparticles on the nanofibers. The stable silica deposition created secondary roughness to the pristine membrane, amplifying its wettability

335 from hydrophilicity to superhydrophobicity. Wettability characterizations revealed that the SiO₂@PVA
336 nanofibrous membrane exhibited outstanding “water-loving” and “oil-hating” properties, with in-air
337 instantaneous water adsorption (0.53s) and underwater oil contact / sliding angle of 161.8° / 6.2°,
338 respectively. The as-prepared SUS membrane showed efficient separation performances for both free
339 oil/water mixture and a variety of surfactant-stabilized oil-in-water emulsions. In addition, light oils
340 were more efficiently rejected by the SUS membrane when compared to heavy oils, which
341 underscored the important role of the oil density during the oil/water separation process. Finally, the
342 SUS membrane showed robust reusability that it maintained stable oil rejection and permeate flux in
343 cyclic experiments.

344

345 **Acknowledgements**

346 The present study was funded by the Joint Research Scheme from National Natural Science
347 Foundation of China and Research Grants Council of Hong Kong under award No. of N_HKU706/16.

348

349 **References:**

- 350 [1] K. Tazaki, A. Fukuyama, F. Tazaki, Y. Shintaku, K. Nakamura, T. Takehara, Y. Katsura, K. Shimada, Twenty Years
351 after the Nakhodka Oil Spill Accident in the Sea of Japan, How Has Contamination Changed?, *Minerals*, 8 (2018) 178.
352 [2] Y. Han, I.M. Nambi, T.P. Clement, Environmental impacts of the Chennai oil spill accident—A case study, *Science of*
353 *the total environment*, 626 (2018) 795-806.
354 [3] Y. Zhu, D. Wang, L. Jiang, J. Jin, Recent progress in developing advanced membranes for emulsified oil/water
355 separation, *NPG Asia Materials*, 6 (2014) e101-e101.
356 [4] W. Qing, X. Shi, Y. Deng, W. Zhang, J. Wang, C.Y. Tang, Robust superhydrophobic-superoleophilic
357 polytetrafluoroethylene nanofibrous membrane for oil/water separation, *Journal of Membrane Science*, 540 (2017) 354-
358 361.
359 [5] L. Yu, M. Han, F. He, A review of treating oily wastewater, *Arabian journal of chemistry*, 10 (2017) S1913-S1922.
360 [6] H. Lin, W. Gao, F. Meng, B.-Q. Liao, K.-T. Leung, L. Zhao, J. Chen, H. Hong, Membrane bioreactors for industrial
361 wastewater treatment: a critical review, *Critical reviews in environmental science and technology*, 42 (2012) 677-740.
362 [7] T. Tong, K.H. Carlson, C.A. Robbins, Z. Zhang, X. Du, Membrane-based treatment of shale oil and gas wastewater:
363 The current state of knowledge, *Frontiers of Environmental Science & Engineering*, 13 (2019) 63.
364 [8] Z. Xue, Y. Cao, N. Liu, L. Feng, L. Jiang, Special wettable materials for oil/water separation, *Journal of Materials*
365 *Chemistry A*, 2 (2014) 2445-2460.

366 [9] Q. Ma, H. Cheng, A.G. Fane, R. Wang, H. Zhang, Recent development of advanced materials with special
 367 wettability for selective oil/water separation, *Small*, 12 (2016) 2186-2202.

368 [10] S. Shao, Y. Liu, D. Shi, W. Qing, W. Fu, J. Li, Z. Fang, Y. Chen, Control of organic and surfactant fouling using
 369 dynamic membranes in the separation of oil-in-water emulsions, *Journal of colloid and interface science*, (2019).

370 [11] S. Zarghami, T. Mohammadi, M. Sadrzadeh, B. Van der Bruggen, Superhydrophilic and underwater
 371 superoleophobic membranes-A review of synthesis methods, *Progress in Polymer Science*, (2019) 101166.

372 [12] L. Yan, G. Zhang, L. Zhang, W. Zhang, J. Gu, Y. Huang, J. Zhang, T. Chen, Robust construction of underwater
 373 superoleophobic CNTs/nanoparticles multifunctional hybrid membranes via interception effect for oily wastewater
 374 purification, *Journal of membrane science*, 569 (2019) 32-40.

375 [13] H. Shi, Y. He, Y. Pan, H. Di, G. Zeng, L. Zhang, C. Zhang, A modified mussel-inspired method to fabricate TiO₂
 376 decorated superhydrophilic PVDF membrane for oil/water separation, *Journal of membrane science*, 506 (2016) 60-70.

377 [14] Y. Cao, W. Zhang, B. Li, P. Wang, L. Feng, Y. Wei, Mussel-inspired Ag nanoparticles anchored sponge for
 378 oil/water separation and contaminants catalytic reduction, *Separation and Purification Technology*, 225 (2019) 18-23.

379 [15] F. Zhang, S. Gao, Y. Zhu, J. Jin, Alkaline-induced superhydrophilic/underwater superoleophobic polyacrylonitrile
 380 membranes with ultralow oil-adhesion for high-efficient oil/water separation, *Journal of membrane science*, 513 (2016)
 381 67-73.

382 [16] F. Sun, W. Liu, Z. Dong, Y. Deng, Underwater superoleophobicity cellulose nanofibril aerogel through
 383 regioselective sulfonation for oil/water separation, *Chemical Engineering Journal*, 330 (2017) 774-782.

384 [17] X. Yang, H. Sun, A. Pal, Y. Bai, L. Shao, Biomimetic Silicification on Membrane Surface for Highly Efficient
 385 Treatments of Both Oil-in-Water Emulsion and Protein Wastewater, *ACS Applied Materials & Interfaces*, 10 (2018)
 386 29982-29991.

387 [18] Z. Wang, S. Ji, F. He, M. Cao, S. Peng, Y. Li, One-step transformation of highly hydrophobic membranes into
 388 superhydrophilic and underwater superoleophobic ones for high-efficiency separation of oil-in-water emulsions, *Journal*
 389 *of Materials Chemistry A*, 6 (2018) 3391-3396.

390 [19] X.-M. Li, D. Reinhoudt, M. Crego-Calama, What do we need for a superhydrophobic surface? A review on the
 391 recent progress in the preparation of superhydrophobic surfaces, *Chemical Society Reviews*, 36 (2007) 1350-1368.

392 [20] Y. Zhu, F. Zhang, D. Wang, X.F. Pei, W. Zhang, J. Jin, A novel zwitterionic polyelectrolyte grafted PVDF
 393 membrane for thoroughly separating oil from water with ultrahigh efficiency, *Journal of Materials Chemistry A*, 1
 394 (2013) 5758-5765.

395 [21] F.E. Ahmed, B.S. Lalia, N. Hilal, R. Hashaikheh, Underwater superoleophobic cellulose/electrospun PVDF-HFP
 396 membranes for efficient oil/water separation, *Desalination*, 344 (2014) 48-54.

397 [22] W. Zhang, Y. Zhu, X. Liu, D. Wang, J. Li, L. Jiang, J. Jin, Salt - induced fabrication of superhydrophilic and
 398 underwater superoleophobic PAA - g - PVDF membranes for effective separation of oil - in - water emulsions,
 399 *Angewandte Chemie International Edition*, 53 (2014) 856-860.

400 [23] X. Zhao, N. Jia, L. Cheng, L. Liu, C. Gao, Dopamine-induced biomimetic mineralization for in situ developing
 401 antifouling hybrid membrane, *Journal of Membrane Science*, 560 (2018) 47-57.

402 [24] Y. Zhu, J. Wang, F. Zhang, S. Gao, A. Wang, W. Fang, J. Jin, Zwitterionic Nanohydrogel Grafted PVDF
 403 Membranes with Comprehensive Antifouling Property and Superior Cycle Stability for Oil - in - Water Emulsion
 404 Separation, *Advanced Functional Materials*, 28 (2018) 1804121.

405 [25] J. Ge, D. Zong, Q. Jin, J. Yu, B. Ding, Biomimetic and superwetable nanofibrous skins for highly efficient
 406 separation of oil - in - water emulsions, *Advanced Functional Materials*, 28 (2018) 1705051.

407 [26] Z. Xu, Y. Zhao, H. Wang, X. Wang, T. Lin, A Superamphiphobic Coating with an Ammonia - Triggered Transition
 408 to Superhydrophilic and Superoleophobic for Oil-Water Separation, *Angewandte Chemie International Edition*, 54
 409 (2015) 4527-4530.

410 [27] P. Gao, Z. Liu, D.D. Sun, W.J. Ng, The efficient separation of surfactant-stabilized oil-water emulsions with a

flexible and superhydrophilic graphene–TiO₂ composite membrane, *Journal of Materials Chemistry A*, 2 (2014) 14082-14088.

[28] J. Ju, T. Wang, Q. Wang, Superhydrophilic and underwater superoleophobic PVDF membranes via plasma-induced surface PEGDA for effective separation of oil-in-water emulsions, *Colloids and Surfaces A: Physicochemical and Engineering Aspects*, 481 (2015) 151-157.

[29] J. Wang, L.a. Hou, K. Yan, L. Zhang, Q.J. Yu, Polydopamine nanocluster decorated electrospun nanofibrous membrane for separation of oil/water emulsions, *Journal of Membrane Science*, 547 (2018) 156-162.

[30] J.-X. Wu, J. Zhang, Y.-L. Kang, G. Wu, S.-C. Chen, Y.-Z. Wang, Reusable and recyclable superhydrophilic electrospun nanofibrous membranes with in situ co-cross-linked polymer–chitin nanowhisker network for robust oil-in-water emulsion separation, *ACS Sustainable Chemistry & Engineering*, 6 (2017) 1753-1762.

[31] W. Zhang, Nanoparticle aggregation: principles and modeling, in: *Nanomaterial*, Springer, 2014, pp. 19-43.

[32] J. Cao, Y. Su, Y. Liu, J. Guan, M. He, R. Zhang, Z. Jiang, Self-assembled MOF membranes with underwater superoleophobicity for oil/water separation, *Journal of Membrane Science*, 566 (2018) 268-277.

[33] L.V. Thomas, U. Arun, S. Remya, P.D. Nair, A biodegradable and biocompatible PVA–citric acid polyester with potential applications as matrix for vascular tissue engineering, *Journal of Materials Science: Materials in Medicine*, 20 (2009) 259.

[34] A.K. An, J. Guo, E.-J. Lee, S. Jeong, Y. Zhao, Z. Wang, T. Leiknes, PDMS/PVDF hybrid electrospun membrane with superhydrophobic property and drop impact dynamics for dyeing wastewater treatment using membrane distillation, *Journal of Membrane Science*, 525 (2017) 57-67.

[35] W. Qing, X. Shi, W. Zhang, J. Wang, Y. Wu, P. Wang, C.Y. Tang, Solvent-thermal induced roughening: A novel and versatile method to prepare superhydrophobic membranes, *Journal of Membrane Science*, 564 (2018) 465-472.

[36] Y. Gu, J. Yang, S. Zhou, A facile immersion-curing approach to surface-tailored poly (vinyl alcohol)/silica underwater superoleophobic coatings with improved transparency and robustness, *Journal of Materials Chemistry A*, 5 (2017) 10866-10875.

[37] H.S. Mansur, C.M. Sadahira, A.N. Souza, A.A. Mansur, FTIR spectroscopy characterization of poly (vinyl alcohol) hydrogel with different hydrolysis degree and chemically crosslinked with glutaraldehyde, *Materials Science and Engineering: C*, 28 (2008) 539-548.

[38] C. Wei, F. Dai, L. Lin, Z. An, Y. He, X. Chen, L. Chen, Y. Zhao, Simplified and robust adhesive-free superhydrophobic SiO₂-decorated PVDF membranes for efficient oil/water separation, *Journal of membrane science*, 555 (2018) 220-228.

[39] Y.-X. Huang, Z. Wang, D. Hou, S. Lin, Coaxially electrospun super-amphiphobic silica-based membrane for anti-surfactant-wetting membrane distillation, *Journal of Membrane Science*, 531 (2017) 122-128.

[40] Z. Peng, L.X. Kong, S.D. Li, Thermal properties and morphology of a poly (vinyl alcohol)/silica nanocomposite prepared with a self - assembled monolayer technique, *Journal of applied polymer science*, 96 (2005) 1436-1442.

[41] H. Ikeda, S. Fujino, T. Kajiwar, Preparation of SiO₂–PVA nanocomposite and monolithic transparent silica glass by sintering, *Journal of the Ceramic Society of Japan*, 119 (2011) 65-69.

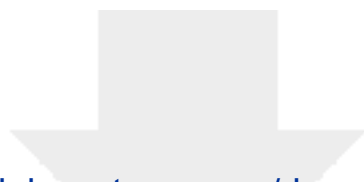
[42] M.A. Gondal, M.S. Sadullah, M.A. Dastageer, G.H. McKinley, D. Panchanathan, K.K. Varanasi, Study of factors governing oil–water separation process using TiO₂ films prepared by spray deposition of nanoparticle dispersions, *ACS applied materials & interfaces*, 6 (2014) 13422-13429.

[43] J. Ge, Q. Jin, D. Zong, J. Yu, B. Ding, Biomimetic multilayer nanofibrous membranes with elaborated superwettability for effective purification of emulsified oily wastewater, *ACS applied materials & interfaces*, 10 (2018) 16183-16192.

[44] M. Padaki, R. Surya Murali, M.S. Abdullah, N. Misdan, A. Moslehyani, M.A. Kassim, N. Hilal, A.F. Ismail, Membrane technology enhancement in oil–water separation. A review, *Desalination*, 357 (2015) 197-207.

[45] A. Salahi, T. Mohammadi, A. Rahmat Pour, F. Rekabdar, Oily wastewater treatment using ultrafiltration,

456 Desalination and Water Treatment, 6 (2009) 289-298.
457 [46] Y. Zhu, D. Chen, Novel clay-based nanofibrous membranes for effective oil/water emulsion separation, Ceramics
458 International, 43 (2017) 9465-9471.
459 [47] J. Zhang, F. Zhang, A. Wang, Y. Lu, J. Li, Y. Zhu, J. Jin, Zwitterionic Nanofibrous Membranes with a Superior
460 Antifouling Property for Gravity-Driven Crude Oil-in-Water Emulsion Separation, Langmuir, 35 (2019) 1682-1689.
461 [48] M. Tian, Y. Liao, R. Wang, Engineering a superwetting thin film nanofibrous composite membrane with excellent
462 antifouling and self-cleaning properties to separate surfactant-stabilized oil-in-water emulsions, Journal of Membrane
463 Science, 596 (2020) 117721.
464



[Click here to access/download](#)

e-Component/supplementary file
Supporting information.docx

